PROCEEDINGS OF SCIENCE

Background Rejection for the ALPHA-g Anti-Hydrogen Detectors

Gareth Smith[a,b,*] **for the ALPHA collaboration**

[a] *TRIUMF,*
4004 Wesbrook Mall, Vancouver, BC, Canada
[b] *The University of British Columbia*
6200 University Blvd, Vancouver, BC, Canada

E-mail: gsmith@triumf.ca

The ALPHA-g experiment recently made the news for the first direct measurement of the gravitational free-fall of anti-hydrogen [1]. Crucial to this milestone is a detector system capable of accurately recording the vertical position of annihilating anti-atoms, with two critical requirements: precise localization of anti-hydrogen annihilations into the "up" or "down" regions, and effective discrimination against the cosmic ray background. To accomplish this, the annihilation products are tracked using a radial time projection chamber detector, and fitted to a common vertex. Simultaneously, a secondary barrel scintillator detector records the time of flight (ToF) of these products. This timing information is used as part of a multivariate analysis to reject externally incident cosmic rays. This presentation showcases the cosmic ray background rejection used in the published measurement, as well as the calibration and analysis campaign to unlock ToF-based background rejection for forthcoming ALPHA-g measurements of the gravitational behavior of anti-hydrogen.

International Conference on Exotic Atoms and Related Topics and Conference on Low Energy Antiprotons
26-30 August 2024
Austrian Academy of Sciences, Vienna, Austria

*Speaker

PoS(EXA-LEAP2024)084

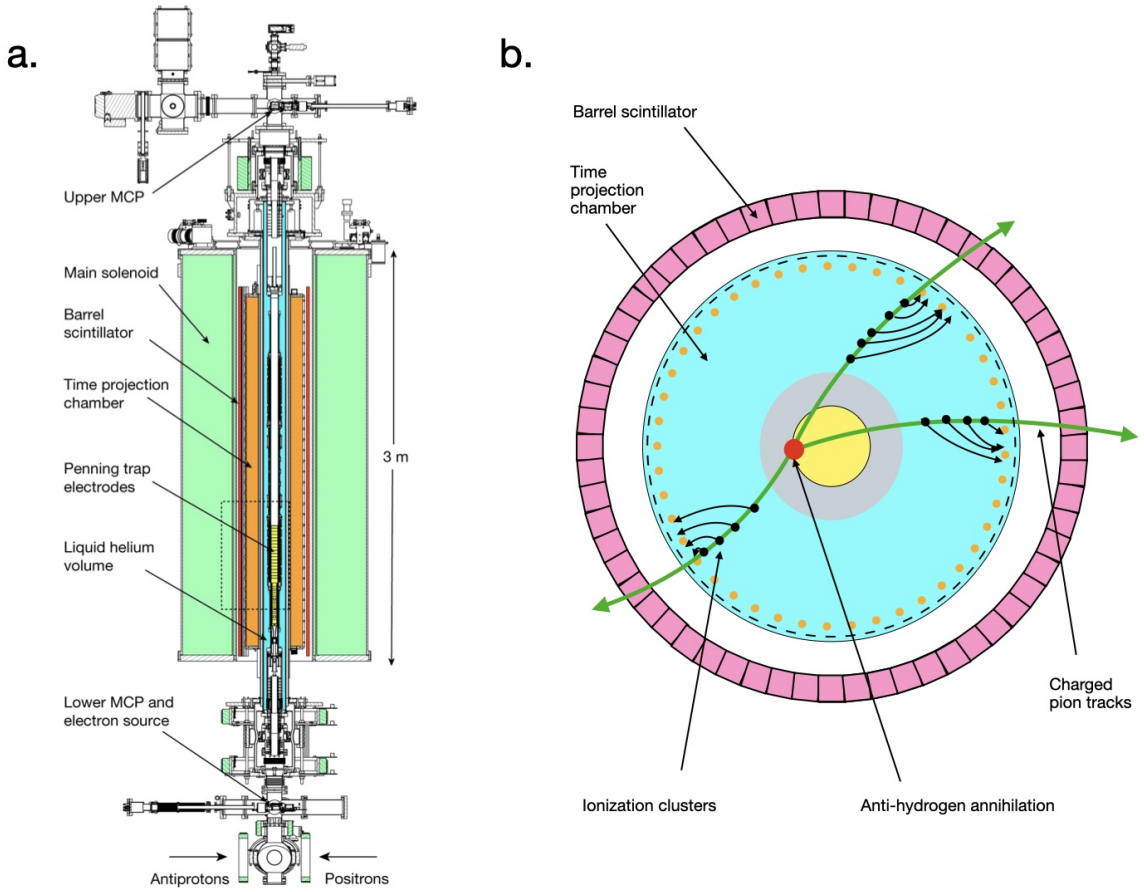

Figure 1: a. An overview of the ALPHA-g apparatus taken from [1]. b. A diagram of an annihilation as seen by the ALPHA-g time projection chamber (blue) and barrel scintillator (pink).

1. Introduction

The ALPHA collaboration at CERN leads the study of trapped anti-atoms. Since first trapping anti-hydrogen atoms in 2010 [2], ALPHA has used the ALPHA-2 apparatus for spectroscopic measurements such as characterizations of the 1S-2S transition [3] and hyperfine splitting [4], and has demonstrated laser cooling of anti-hydrogen [5]. These achievements advance ALPHA's goal of verifying CPT symmetry by comparing matter and anti-matter atoms. While spectroscopical developments with ALPHA-2 continue, the collaboration has turned towards another fundamental symmetry which anti-matter is believed to follow: Einstein's weak equivalence principle. A new ALPHA-g apparatus was designed to demonstrate that gravity has an equivalent effect on matter and anti-matter.

Existing ALPHA infrastructure is used to create anti-proton and positron plasmas inside the ALPHA-g Penning-Malmberg trap, pictured in Fig.1a. The two plasmas are combined, and the low-field seeking anti-hydrogen atoms produced with the lowest energy are trapped by a superimposed magnetic trap. Once a sufficient sample of anti-atoms has been collected, a gravity measurement is performed by ramping down both mirror coils to allow vertical escape while the octupole magnet maintains radial confinement. In the absence of a bias, most anti-atoms escape downwards due to

the effect of gravity; the exact ratio depends on the atom's trajectories and is determined through simulation. A bias can be applied by passing a slightly higher current through one mirror coil. By finding the bias that exactly cancels gravity and restores the up-down ratio to 50-50, the strength of the Earth's gravitational field on anti-hydrogen atoms was measured [1].

2. ALPHA-g Anti-Hydrogen Annihilation Detectors

A key step in this measurement is detecting anti-hydrogen annihilations on the trap wall after they are released from the confining magnetic fields. The detector system must localize the annihilations to "up" and "down" regions separated by 25.6 cm, and have sufficiently low background to detect a few counts over the 20 second magnet ramp. A *radial time projection chamber* (TPC) is the detector of choice, using an argon-CO2 gas mix with a drift region created by a radial electric field. Electron avalanches induce a charge on 256 anode wires and 18432 cathode pads. These signals are digitized and used to reconstruct tracks, and the annihilation position is determined as the point where these tracks pass closest to each other. This process is pictured in Fig.1b, and described elsewhere in these proceedings [6].

Cosmic ray muons create a problematic background for the TPC, triggering the detector at a rate of 70 Hz. To address this, it is surrounded by a secondary *barrel scintillator* (BSC) detector, composed of 64 trapezoidal bars of EJ-200 scintillator [7] of width 2 cm and length 2.6 m. Each bar is read out at each end by an array of six 6 mm x 6 mm Onsemi/Sens-L J-series silicon photomultipliers (SiPMs) [8]. Whereas electrons drift for many µs in the TPC, the barrel scintillator takes only a few ns for photon and travel and signal generation by the SiPMs. The signal times at both ends of the bar are combined to determine both the vertical z position and the time of the hit. When matched with TPC tracks, these hit times give the ability to determine the direction of a charged particle track. This allows for discrimination between externally incident particles with one inbound and one outbound track, and annihilation events with many outbound tracks.

3. Barrel Scintillator Precision Timing

Readout of the BSC proceeds uses circuit boards developed at TRIUMF which perform an analog sum of the six SiPM signals from each bar end. The signal path is split into two branches. One branch passes through a pulse shaper and is sampled by a custom Analog-to-Digital Converter (ADC) [9]. The other is converted to a digital signal by means of a programmable voltage comparator, and digitized by a TRB3 Time-to-Digital Converter (TDC) [10]. The TDC achieves a time resolution much shorter than a 5 ns clock cycle by passing the incoming signal through a delay chain. Each element of the delay chain has a characteristic delay time, which must be determined using a few hours of cosmic ray data. This calibration, known as the fine time calibration, is very stable and should be repeated approximately yearly.

3.1 Channel offset correction

A further calibration corrects for individual channel time delay due to, for example, signal propagation through differing cable lengths. Ideally, a generated pulse applied to the start of the signal path would easily quantify this effect. However, a number of unforeseen issues prevented

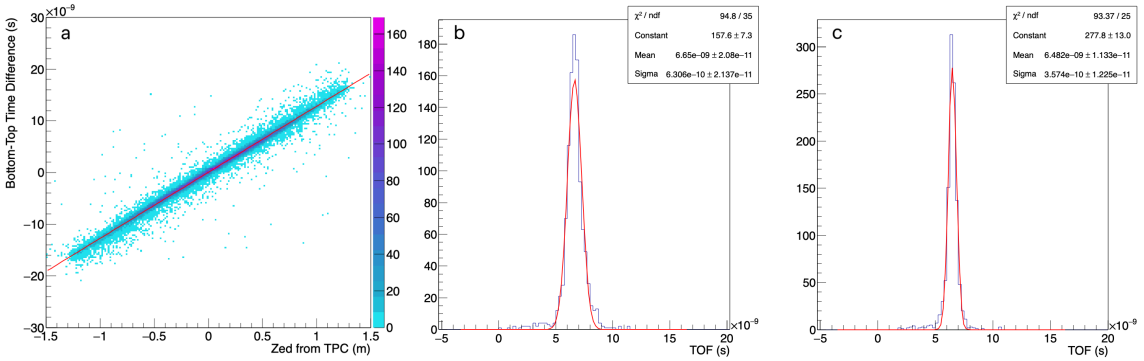

Figure 2: a. Plot of TDC top-bottom time difference against z position from TPC, used to extract top-bottom offset and effective speed of light in bar. b. The ToF between one bar and another roughly opposite, with no time walk correction applied, fit with a Gaussian. c. The same ToF distribution, with a time walk correction applied which minimizes the width of the Gaussian fit.

this approach. The pulse generation and distribution circuit proved unreliable, and the magnitude of this effect was much larger than expected, with the TDC itself contributing offsets of tens of ns to each channel. These offsets would change completely when the TDC was rebooted. Due to a problem with the clock input, the TDC would crash sporadically, causing these offsets to change as often as every few days. These issues ruled out a traditional once-per-year calibration using a pulse generator. Instead, an algorithm was developed to calibrate these offsets using cosmic ray data already routinely collected. This algorithm currently runs automatically in the background, providing an up-to-date online calibration after every run. Offline, the same algorithm is used to produce the most precise calibration.

The correction algorithm starts by finding the time offset between the top and bottom of a bar. Bar hits are matched to TPC tracks, which are extrapolated to the BSC radius. The SiPM signal time difference between the two ends of the bar is plotted against the z position given by the TPC; see Fig.2a. for example. The Y-intercept of this plot is interpreted as the offset between top and bottom, and the slope is similarly interpreted as an effective speed of light in the bar.

Next, the offset between every pair of two bars is determined. Neighboring bar hits are grouped into clusters, and events with four or more clusters were excluded to ensure a pure sample of cosmic ray events. For every combination of two bar hits, the time difference between hits was plotted and the mean offset extracted from a Gaussian fit. The first hit was defined as the one with the higher z position, leveraging the fact that cosmic rays originate from above due to the Earth's shielding.

After extracting the offsets between pairs of bars, a characteristic offset for each bar can be determined. The offset t_i for bar i can be calculated from the offsets $d_{i,j}$ to the other bars j as:

$$t_i = \frac{1}{|G_i|} \sum_{j \in G_i} d_{i,j} + \frac{1}{|G_i|} \sum_{j \in G_i} t_j \tag{1}$$

Here, G_i is the subset of bars for which the bar-to-bar offsets were measured properly, excluding failed fits, and low statistics, and dead channels. This equation is not exactly solvable, and so an iterative numerical approach was used.

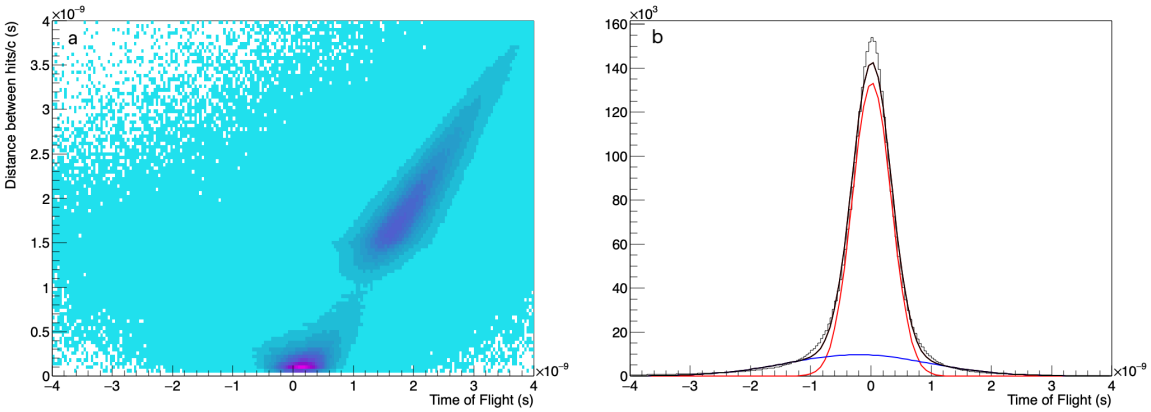

Figure 3: a. The final cosmic ray ToF plotted against the physical distance between the two BSC hits. b. The time of flight residuals, i.e. the diagonal projection of a. It is fit with a double Gaussian.

3.2 Time walk correction

Two pulses with the same shape cross a fixed threshold at a different time depending on their sizes; a larger amplitude pulse will cross the threshold sooner. This effect is known as the time walk effect, and must be accounted for to obtain a true SiPM signal start time. Our approach was to correct for this effect in analysis, measuring the amplitude of each pulse with an ADC. If the signal is saturated, the amplitude is recovered from a fit to the unsaturated part of the pulse.

The traditional approach to this calibration is to determine the relationship between signal amplitude and hit time by averaging over a large quantity of data. However, this approach requires a well-defined zero time, such as from a bunch crossing in collider experiments, which is not available for ALPHA-g. Furthermore, issues with the pulse generation and distribution prohibits performing such a calibration with generated pulses. The approach taken was to assume a form $\delta t = k/\sqrt{A}$ for the time walk correction, where A is the measured amplitude. This is exact for a pulse with a quadratic rise, which matches the SiPM signals we observe. The values of the constant k were determined individually for each bar end using cosmic ray data. For each bar, a second bar was chosen, usually the geometrically opposite bar. The distribution of cosmic ray ToF between those two bars was populated, again with the higher-z hit as the first one. The value of k was simultaneously optimized for the four bar ends in order to minimize the width of this distribution, as shown in Fig.2b and c. In subsequent analysis, the BSC hit time is then determined as:

$$t = \left(t_{\text{top}} + \delta t_{\text{top},i} + t_{\text{bot}} + \delta t_{\text{bot},i}\right)/2 + t_i \tag{2}$$

where t_{top} is the measured top SiPM hit time including the fine time calibration, δt is the time walk correction descried above, and t_i is the characteristic bar offset. The measured cosmic ray ToF is compared to an ideal ToF calculated using the distance between the two hits and assuming $v = c$, as shown in Fig.3. The residual ToF is fit with a double Gaussian, and the inner Gaussian sigma of 322 ps is taken as the time resolution.

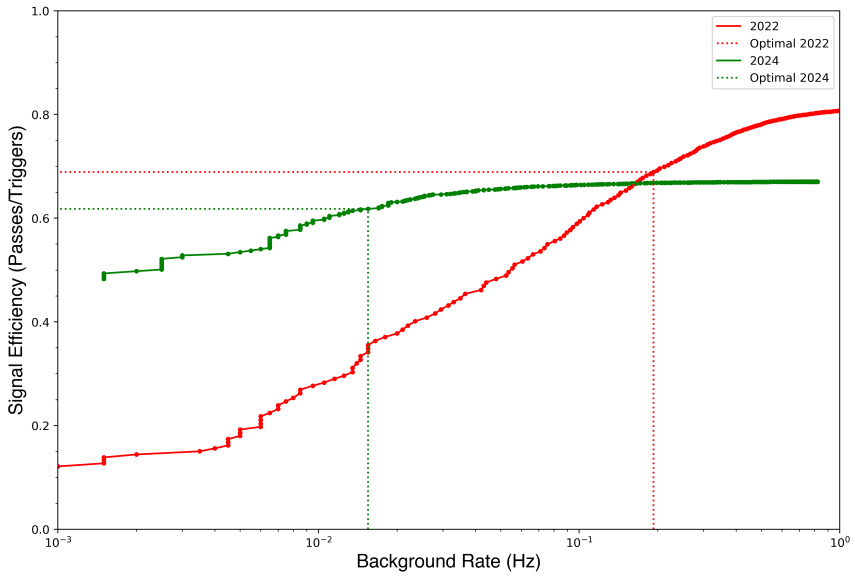

Figure 4: Background rate vs. signal efficiency curve comparison between the MVA used in [1], and the new 2024 MVA including ToF. Dotted lines indicate the chosen working points.

4. Multivariate Analysis for Background Rejection

For the gravity analysis in [1], a multivariate analysis (MVA) using ROOT's Toolkit for Multivariate Analysis (TMVA) [11] was trained to distinguish between cosmic ray background events and anti-hydrogen annihilations. This relied primarily on variables from the TPC, such as the number and density of spacepoints, or the number and direction of tracks. It also included some topological information from the BSC, such as the number of hits or clusters of hits. Boosted decision trees were trained on 371,362 signal events and 611,942 background events. This analysis was able to decrease the cosmic ray background by a factor of 350 to around 0.2 Hz.

With the BSC time corrections in place, ToF information is now included in the MVA. A new analysis was trained; of the 20 most sensitive variables, 6 use the calibrated ToF information, and 15 involve the BSC. This improved MVA has lead to a further order of magnitude improvement, with a final background rate of around 0.015 Hz. This is shown in Fig.4.

5. Conclusions

In 2023, ALPHA-g published the first measurement of the gravitation acceleration of anti-hydrogen atoms. Key to this milestone were the ALPHA-g detectors, which detected the few hundred annihilating anti-atoms amid a large background of cosmic rays. The time calibrations presented here unlock the capabilities of the BSC detector to identify the direction and ToF of annihilation products, drastically improving background rejection and reducing associated uncertainties. Furthermore, this opens the door to new techniques which might require observation of annihilations over a much longer period.

References

[1] E. Anderson, C. Baker, W. Bertsche et al., *Observation of the effect of gravity on the motion of antimatter*, *Nature* **621** (2023) 716.

[2] G. Andresen, M. Ashkezari, M. Baquero-Ruiz et al., *Trapped antihydrogen*, *Nature* **468** (2010) 673.

[3] M. Ahmadi, B. Alves, C. Baker et al., *Observation of the 1s–2s transition in trapped antihydrogen*, *Nature* **541** (2017) 506.

[4] M. Ahmadi, B. Alves, C. Baker et al., *Observation of the hyperfine spectrum of antihydrogen*, *Nature* **548** (2017) 66.

[5] C. Baker, W. Bertsche, A. Capra et al., *Laser cooling of antihydrogen atoms*, *Nature* **592** (2021) 35.

[6] A. Capra, *Antihydrogen annihilation detection: the ALPHA-g radial TPC*, in *Proceedings of the International Conference on Exotic Atoms and Related Topics and Conference on Low Energy Antiprotons*, PoS(EXA-LEAP2024), p. 063, 2024, DOI.

[7] Eljen Technology, *Plastic scintillators ej-200, ej-204, ej-208, ej-212*, 2024.

[8] ON Semiconductor, *MicroJ Series High-Performance Diodes*, 2024.

[9] A. Garnsworthy, C. Pearson, D. Bishop, B. Shaw, J. Smith, M. Bowry et al., *The griffin data acquisition system*, *Nuclear Instruments and Methods in Physics Research Section A: Accelerators, Spectrometers, Detectors and Associated Equipment* **853** (2017) 85.

[10] A. Neiser, J. Adamczewski-Musch, M. Hoek, W. Koenig, G. Korcyl, S. Linev et al., *TRB3: a 264 channel high precision TDC platform and its applications*, *Journal of Instrumentation* **8** (2013) C12043.

[11] A. Hoecker, P. Speckmayer, J. Stelzer, J. Therhaag, E. von Toerne, H. Voss et al., *TMVA - Toolkit for Multivariate Data Analysis*, 2007. 10.48550/arXiv.physics/0703039.

PoS(EXA-LEAP2024)084